

The e-MERGE e-MERLIN/VLA/VLBI Wide-field Deep High Angular Resolution Survey of GOODS-N

Tom Muxlow ^{a*}, Ian Smail ^b, Ian McHardy ^c, Jack Radcliffe ^d, Isabella Prandoni ^e, Ann Ngeri Ng'Endo ^f, and the e-MERGE Consortium

a Jodrell Bank Centre for Astrophysics, Univ. of Manchester, Oxford Road, Manchester M13 9PL, UK

b Centre for Extragalactic Astronomy, Dept. of Physics, Durham University, Durham DH1 3LE, UK

c Department of Physics and Astronomy, The University, Southampton SO17 1BJ, UK

d Department of Physics, University of Pretoria, Lynnwood Road, Hatfield, Pretoria 0083, South Africa

e INAF-Istituto di Radioastronomia, via Gobetti 101, Bologna 40129, Italy

f School of Mathematics, Statistics & Physics, Newcastle University, Newcastle upon Tyne NE1 7RU, UK

E-mail: tom.muxlow@manchester.ac.uk

The initial description paper for the e-MERGE deep ($\sim 1\mu\text{Jy/bm}$), (30x30 arcmin field) high-resolution radio survey of GOODS-N is now published [1]. Images are now available to the e-MERGE consortium from Data Release-1 (DR-1) covering the inner central 15x15 arcmin region. The e-MERGE results demonstrate the ability of high-resolution imaging at 1.5 & 5.5 GHz to spatially resolve regions of radio emission associated with star-formation within the 848 DR-1 catalogued radio sources out to $z=3$ and differentiate such regions from those associated with actively accreting AGN-jet systems.

The DR-2 enhancement is under way utilizing all the e-MERLIN+VLA 1.5GHz (unaveraged) data with imaging out to the full 30x30 arcmin field of view, which will produce a single wide-field image to a depth of $\sim 500\text{nJy/bm}$ in the inner 7.5 arcmin diameter field and $\sim 1\mu\text{Jy/bm}$ in the surrounding outer annulus - a factor of x4 increase in field size and x2 increase in depth in the inner region. An additional 24-hrs of (associated) e-MERGE 1.5GHz data were observed with the EVN [2] providing mas-scale resolution at 582 correlation positions centered on the e-MERLIN field, the vast majority of which lie within the DR-1 area (central sensitivity $\sim 9\mu\text{Jy/bm}$, beam $\sim 5\text{mas}$.)

Initial results for combination EVN+e-MERGE 1.5GHz imaging from a sample of 31 AGN-dominated radio sources are discussed with regard to the majority being compact core + (galactic-scale) extended radio structures, possibly the high-redshift tail to the local Universe FR0-type radio structures [3], the most common form of radio AGN systems found in the Universe.

15th European VLBI Network Mini-Symposium and Users' Meeting (EVN2022)

11-15 July 2022

University College Cork, Ireland

*Speaker

© Copyright owned by the author(s) under the terms of the Creative Commons Attribution-NonCommercial-NoDerivatives 4.0 International License (CC BY-NC-ND 4.0).

1. Introduction

The initial DR 1 release covering the inner 15x15 arcmin region of e-MERGE with matched resolution e-MERLIN+VLA combination images at 1.5 GHz and VLA at 5.5 GHz have demonstrated that the radio source population with 1.5GHz flux densities <1mJy is dominated by steep spectrum star-forming galaxies with emission extended on galactic scales. The radio source AGN population consists of radio quiet systems with central cores and one- or two-sided extended emission on galactic scales. Of the 848 catalogued radio source within the e-MERGE DR-1 area only 2 classical AGN double structures found – 1 FRI system and one Wide-Angled Tail.

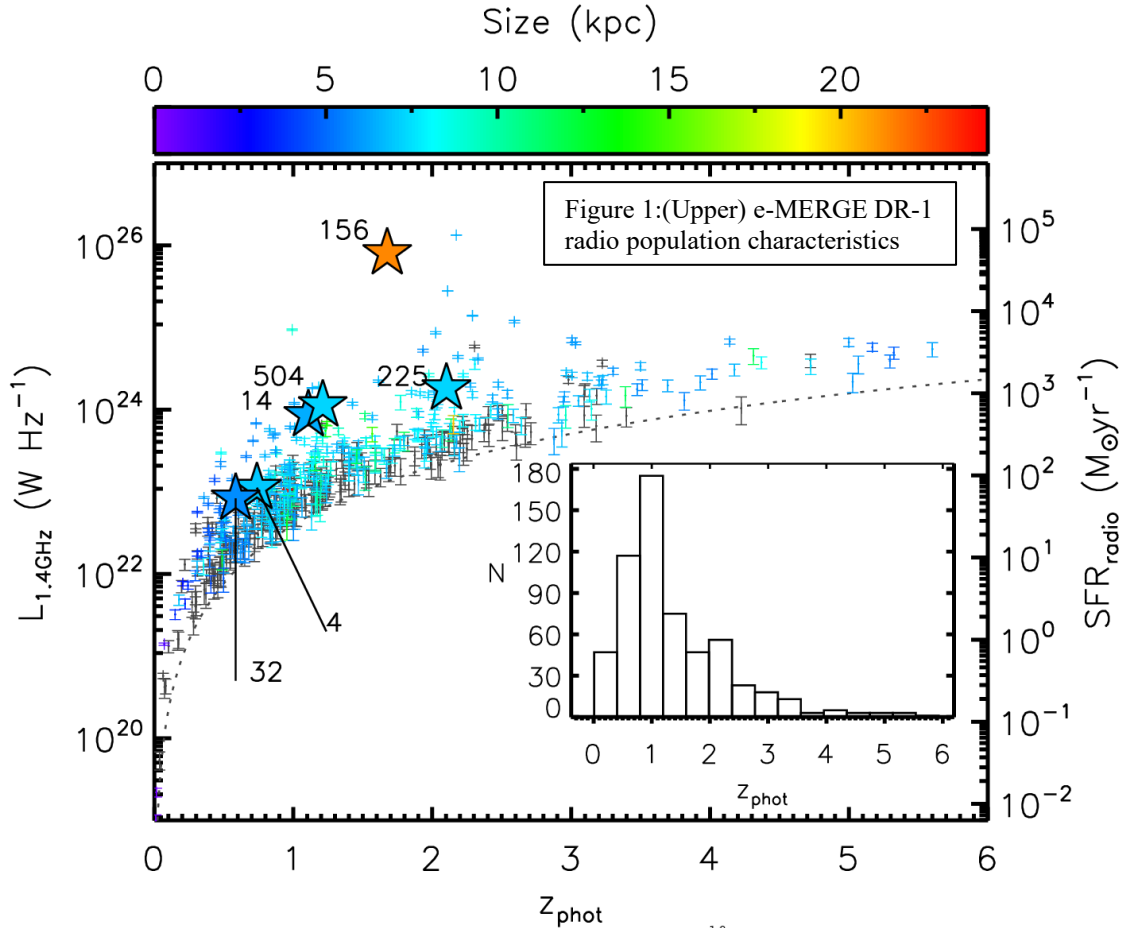


Figure 1 (Upper) shows the properties of the DR-1 catalogued radio source population plotted against L-Band monochromatic radio luminosity, star-formation rate for the identified star-forming galaxies, redshifts (detected $z \leq 6$), and colour-coded linear sizes. The population is dominated by small (<20kpc) high-z systems. The 2 classical radio-loud AGN double sources lie outside the linear size scale shown and are omitted from the figure; Sources with large icons & catalogue numbers are discussed in detail in [1]. Figure 1 (Lower) shows the changing nature of the radio population below an L-Band flux density of 1mJy

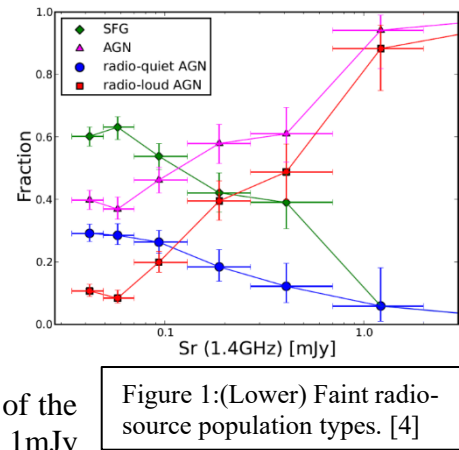


Figure 1:(Lower) Faint radio-source population types. [4]

population with increasing numbers of star-forming galaxies and radio-quiet AGN systems whilst the numbers of radio-loud systems fall rapidly with flux density [4].

2. Science Extraction on AGN e-MERGE Sources

The high angular resolution (~ 200 mas) sensitive imaging ($\sim 1.5\mu\text{Jy}/\text{bm}$) from e-MERGE DR-1 images allows detailed analysis of individual sources and the separation of star-forming systems from low-luminosity Radio-Quiet AGN sources by radio structure morphology and spectral index. ~ 500 of the e-MERGE radio-selected galaxies with optical counterparts have deblended Herschel *SPIRE* IR photometry [5] at matching angular resolution to the radio images. Of these, $\sim 15\%$ of DR-1 population are Radio-Quiet AGN with $q_{\text{IR}} < 1.95$ and extended one- or two-sided galactic scale emission surrounding a low-luminosity AGN core (see Figures 2 and 3).

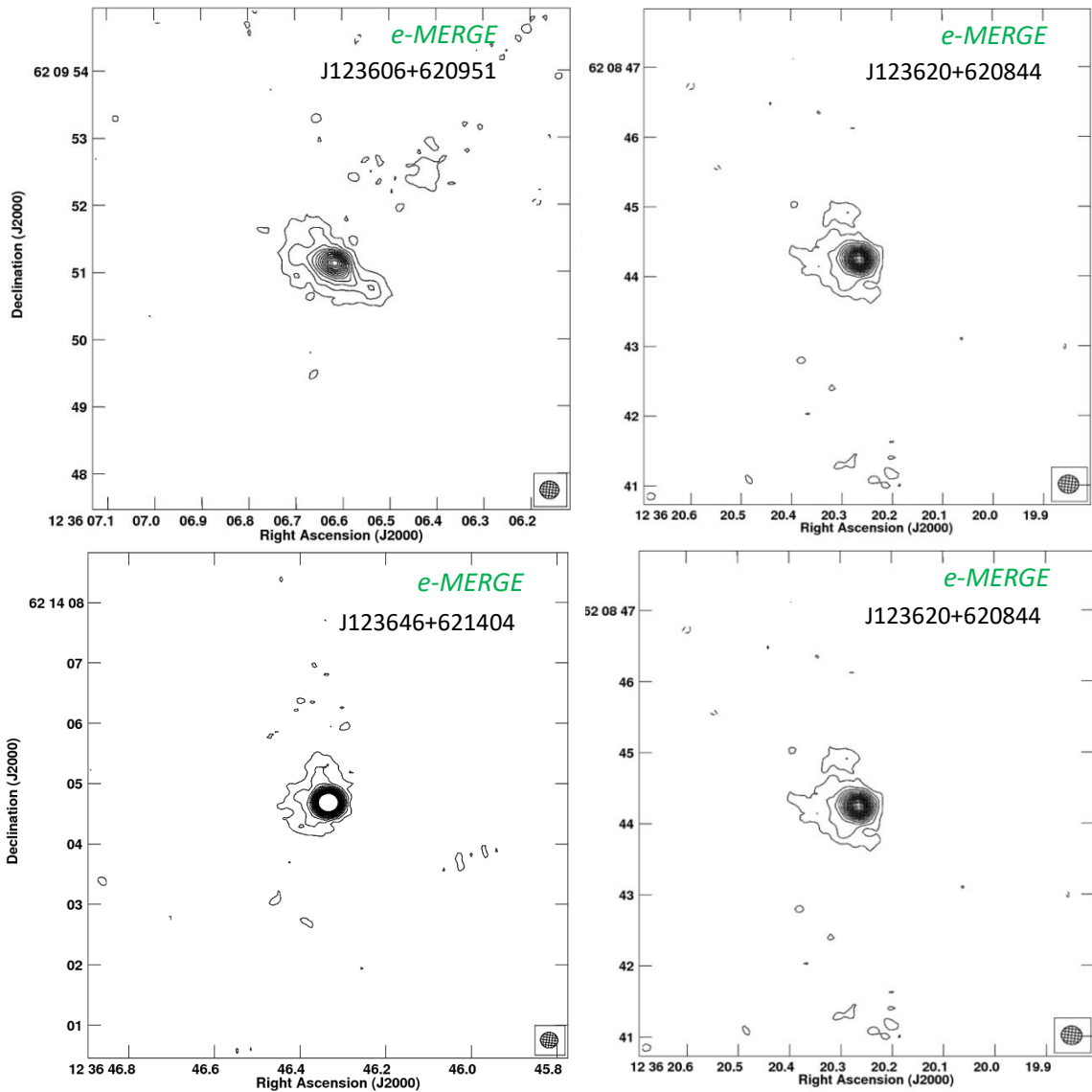


Figure 2: e-MERGE 1.5 GHz images (Beam ~ 200 mas) of 4 example Radio-Quiet AGN systems with compact nuclear components and one- or two-sided extended radio components on galactic scales.

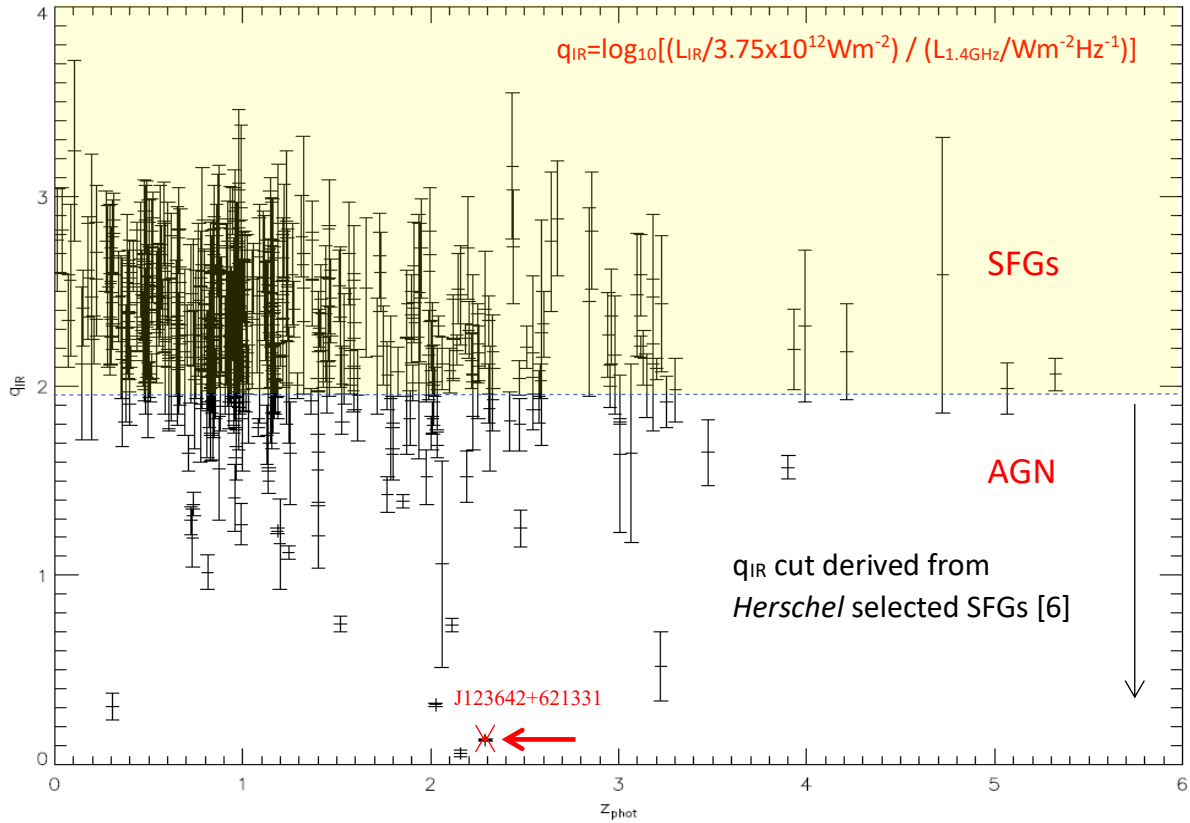


Figure 3: Q_{IR} values obtained from de-blended *Herschel SPIRE* IR photometry for those catalogued DR-1 radio sources with optical counterparts plotted against redshifts. AGN have q_{IR} values < 1.95

The addition of EVN 1.5 GHz data is being used to investigate jet length and sidedness for the radio-quiet AGN radio source population in e-MERGE DR-1. Such studies will separate AGN-jet features from star-forming regions some of which may be the result of AGN feedback interactions. These additional studies are at an early stage and examples of intermediate resolution ($\sim 100\text{mas}$) combination EVN + e-MERGE 1.5GHz images have been made to investigate 2 DR-1 AGNs: Radio-Quiet AGN J123642+621331 and Radio-Loud WAT J123725+621129

2.1 J123642621331 – Radio-Quiet AGN

We have used e-MERGE+EVN 1.5 GHz combination imaging with angular resolutions of 100 mas to study jet length and sidedness of a sub-set of the DR-1 Radio-Quiet AGN population in order to constrain models of SMBH jet launching and investigate SMBH mass and spin in these high-redshift systems through the jet properties close to the AGN cores. A single example Radio-Quiet AGN system at a redshift of is discussed below. The object is confirmed as a Radio- Quiet AGN through its very low q_{IR} value well below the SFG/AGN cut off value of 1.95 (Figure. 3). The source shows a one-sided jet through all of its Easterly length with significant changes in position angle overlying a two-sided lower surface brightness component on a galactic size scale size. (See Figures 4 & 5). The radio structure, if typical, shows that although jets are clearly active in such Radio-Quiet AGN systems at high redshifts, they do not have the power to break out into the extragalactic region – and there are no signs of any jet termination hotspots. For the one-sided/asymmetrical structures either the jets are initially fast-moving and showing evidence of Doppler beaming on the foreground side, or perhaps the jets oscillate back and forth between the

sides and at present only the jet on one side is active. If the jets are initially launched with relativistic motions, they appear to gradually lose their power (and speed) within the surrounding host galaxy since none of the e-MERGE imaged Radio-Quiet AGN systems shows any evidence of jet termination shocks or extended emission beyond the host galaxy.

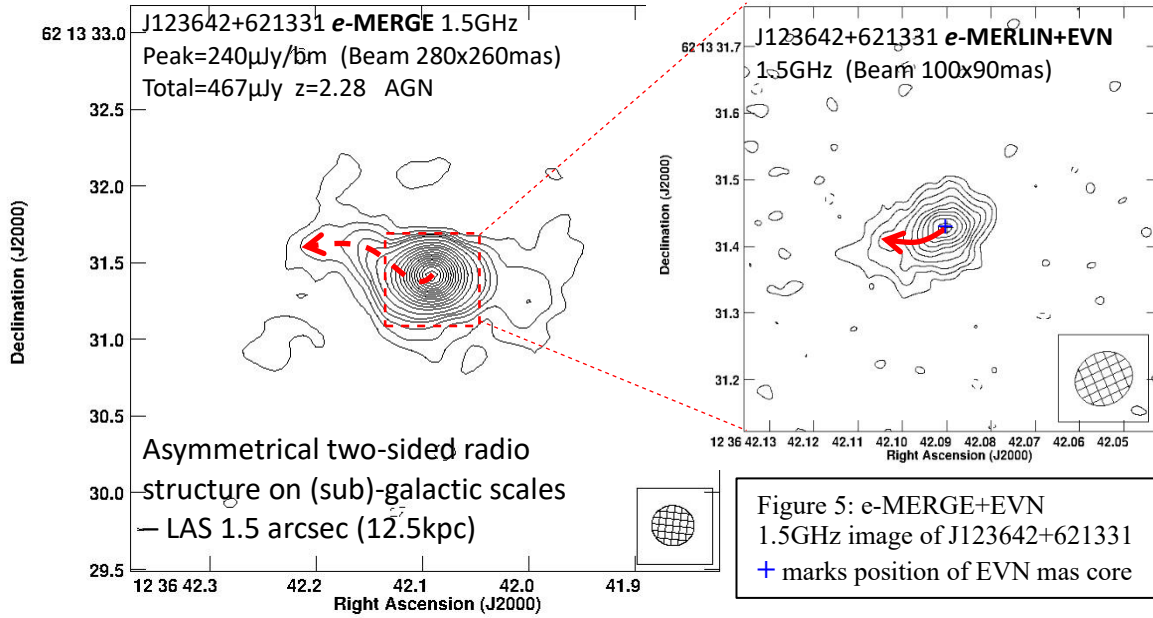


Figure 4: e-MERGE 1.5GHz image of J123642+621331

2.2 J123725 +621129 – Radio-Loud Wide-Angled Tail

The radio core of this Wide-Angled-Tail (WAT) radio source overlies the nucleus of an $I=22.9\text{mag}$ $z=1.2653$ massive elliptical galaxy $M \sim 1.8 \pm 0.1 \times 10^{11} M_{\odot}$. This source is the bright-

est object in the e-MERGE DR-1 release region with a total flux density at 1.5 GHz of 5.5mJy. As with other WAT systems, the collimated jets from the central radio core component are disrupted by the surrounding cluster gas at hotspots located near the edge of the visible galaxy at the Interstellar & Intracluster (ISM/ICM) interface. The disrupted plasma from the jets then drifts out under buoyancy forces into the surrounding hot intra-cluster medium (ICM). Figure 6 shows the VLA A-array 1.5 GHz image in false colour, which maps out the angular extent of the radio source (LAS~4.2 arcseconds). Figure 7 illustrates the significant increase in the detailed radio structure which can be found with the higher angular resolution e-MERLIN 1.5 GHz image shown contoured over the HST F850LP image of the

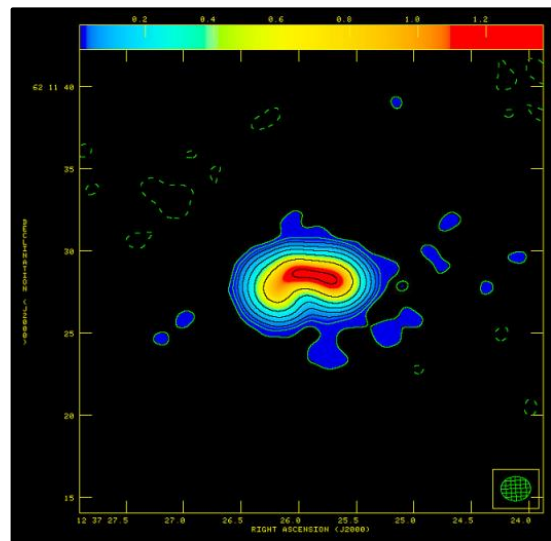


Figure 6: VLA A-array 1.5GHz image of J123725+621129

POS(EVN2022)044

host galaxy in false colour. The increased detail shows that the radio structure is bent significantly out of linearity by the buoyancy forces in the surrounding ICM such that the total extent of the double radio lobed structure is closer to 6 arcseconds ($\sim 50\text{kpc}$ at a redshift of 1.2653).

A spectral index map between 1.5 GHz and 5.5 GHz for the WAT is shown in Figure 8 from matched resolution imaging with the e-MERLIN 1.5 GHz map smoothed to the resolution of the VLA A-array 5.5 GHz image. The core

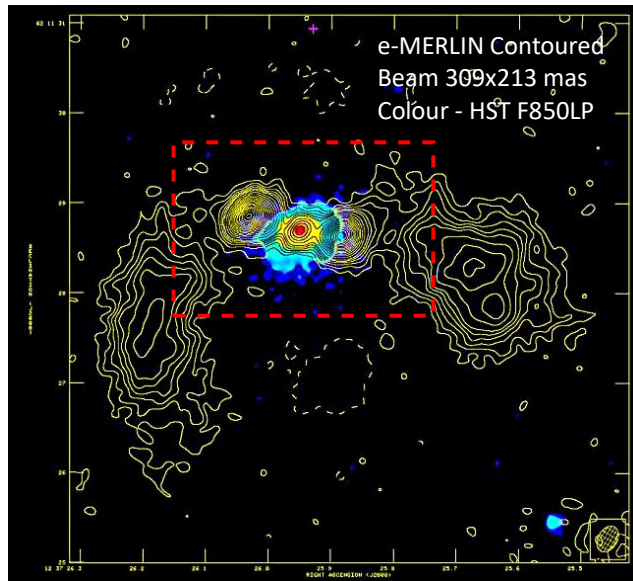
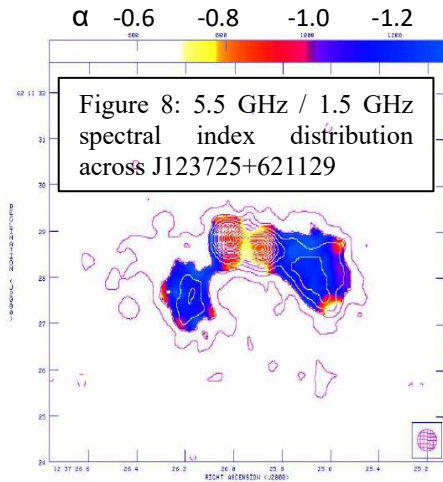
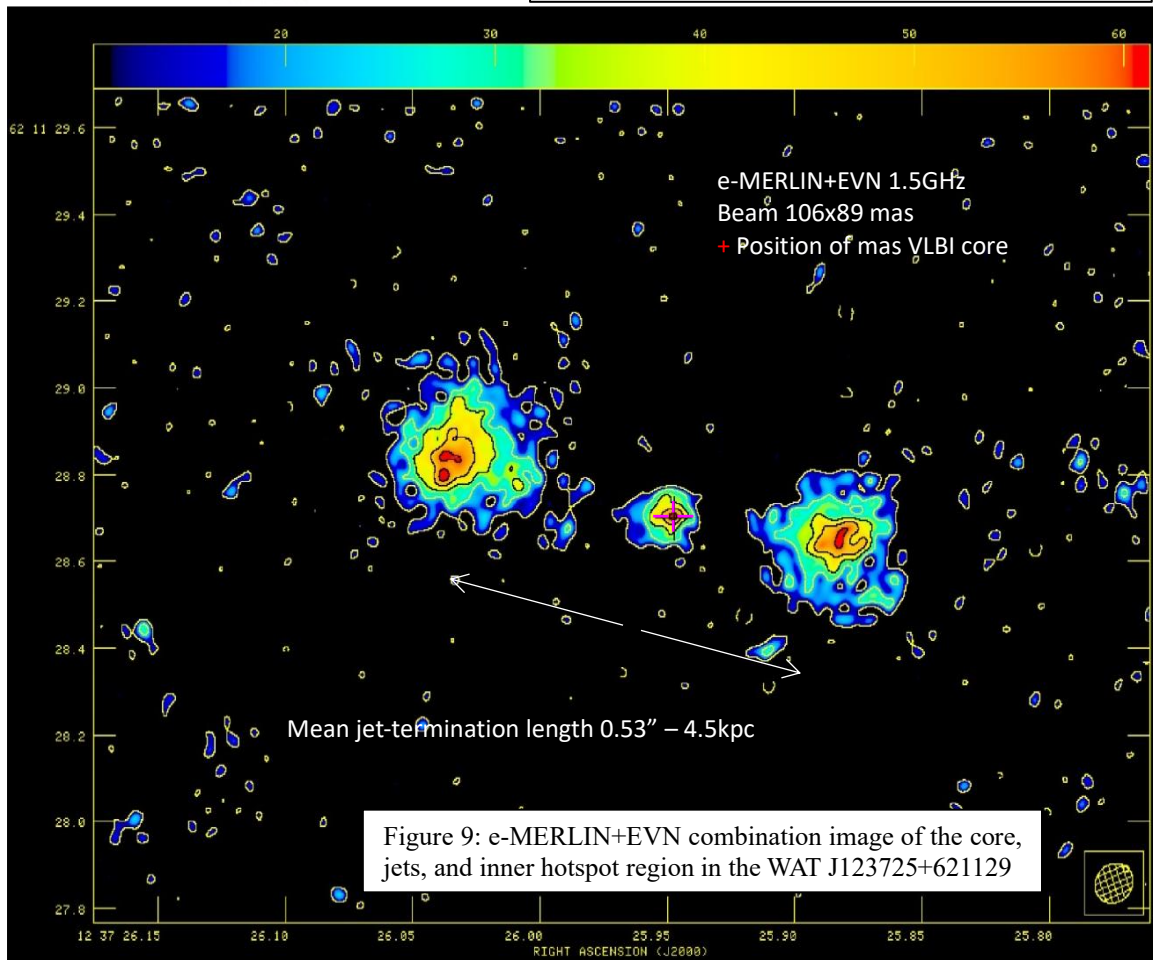


Figure 7: e-MERLIN 1.5GHz image of J123725+621129 contoured over HST F850LP in false colour. The hatched box shows the region imaged in Figure 9.



POS(EVN2022)044

emission shows the flattest radio spectral index with the inner hotspots and outer lobes showing progressively steep spectral indices.

2.2.1 The Properties of WAT J123625+621129.

The overall size of the WAT radio structure after accounting for bending is ~ 50 kpc which is small by comparison with other luminous WAT systems – inviting the question as to whether this is a young object. An estimate of the source age can be made by comparing the spectral indices (α , $S \propto \nu^{-\alpha}$) found between the e-MERGE 1.5 GHz and VLA 5.5 GHz images in the inner hotspot regions ($\alpha = -0.82 \pm 0.04$) and the outer lobe structures ($\alpha = -1.37 \pm 0.12$), assuming that no significant electron acceleration in the plasma occurs beyond the hotspot regions. Ageing of the electron population in the lobes produces a cut-off in the high energy electron population from Synchrotron losses resulting in a steepening in the observed spectrum above a certain critical frequency – as this frequency moves below 5.5 GHz the observed spectral index will steepen allowing an estimate of the plasma age to be estimated provided the magnetic field strength is known [7]. Using a fiducial value of $5 \mu\text{G}$ for the magnetic field strength value in such regions as found in similar structures [8] yields a spectral age of ~ 50 Myr which implies that the radio source is not particularly old. Such spectral age estimates are subject to potential inaccuracies due to, for example, the adiabatic expansion of plasma within the lobes of radio sources [9]. Another energy loss process whose characteristic timescale we can infer from our observations is that of Inverse Compton losses off the radiation field of the AGN itself. Estimates from [15] suggest an Inverse Compton age of ~ 20 Myrs and combinations of both Inverse Compton and adiabatic expansion derives more realistic age estimates of ~ 18 Myr. Such relatively young age estimates suggest that J123725+621129 is likely a rapidly evolving source in the early throes of interacting with the surrounding ICM. That said, J123725+621129 is the brightest source in the DR-1 field (S_{tot} at 1.5GHz = 5.5mJy) and this and other high angular resolution deep surveys have not yet detected any older and larger WAT structures which calls into question whether such young evolving high redshift WAT structures grow into larger and older WATs – or whether they are relatively transitory objects which never live long enough to evolve into larger WAT systems.

Figure 9 shows the e-MERLIN+EVN 1.5GHz combination image of core, jet, and inner hotspot region of the WAT showing the disruption of the jets by their interaction with ICM as they escape the protection of the host galaxy ISM. The jets joining the core to the inner hotspots are clearly visible in the e-MERLIN 1.5 GHz image and are quite symmetrical - but are relatively faint and due to the increased angular resolution and lower sensitivity, are not visible in the EVN combination image aside from the initial Eastward-facing one-sided jet emanating from the core. The average separation between the AGN radio core and the hotspots (the jet termination length) is 0.53 arcseconds (4.5 kpc).

For comparison purposes, we have assembled a compilation of Wide-Angled Tail radio sources from the literature, including (a): a selection of $z \leq 0.5$ WATs located within Abell clusters [10]; (b): 38 WATs between $0 < z < 0.96$ detected in the VLA FIRST survey [11][12][13]; and (c): 6 WATs detected at $0.14 < z < 0.38$ in the Australia Telescope Wide Area Survey [14]. We note that J123725+621129 is at a higher redshift than any other WAT source thus far studied in detail with high angular-resolution radio imaging. Whilst also being of comparable luminosity with typical Wide-Angled Tail sources in the redshift range $\sim 0.5 - 1$, J123725+621129 is very small in linear size being- around $\frac{1}{4}$ the size of typical high redshift WAT systems.

Figure 10 shows the properties of the WAT representative sample in terms of monochromatic luminosity and linear size against redshift. It should be noted that this sample is not complete in any formal sense, but representative of typical WAT structures published in the literature.

Comparison with a Representative WAT Sample

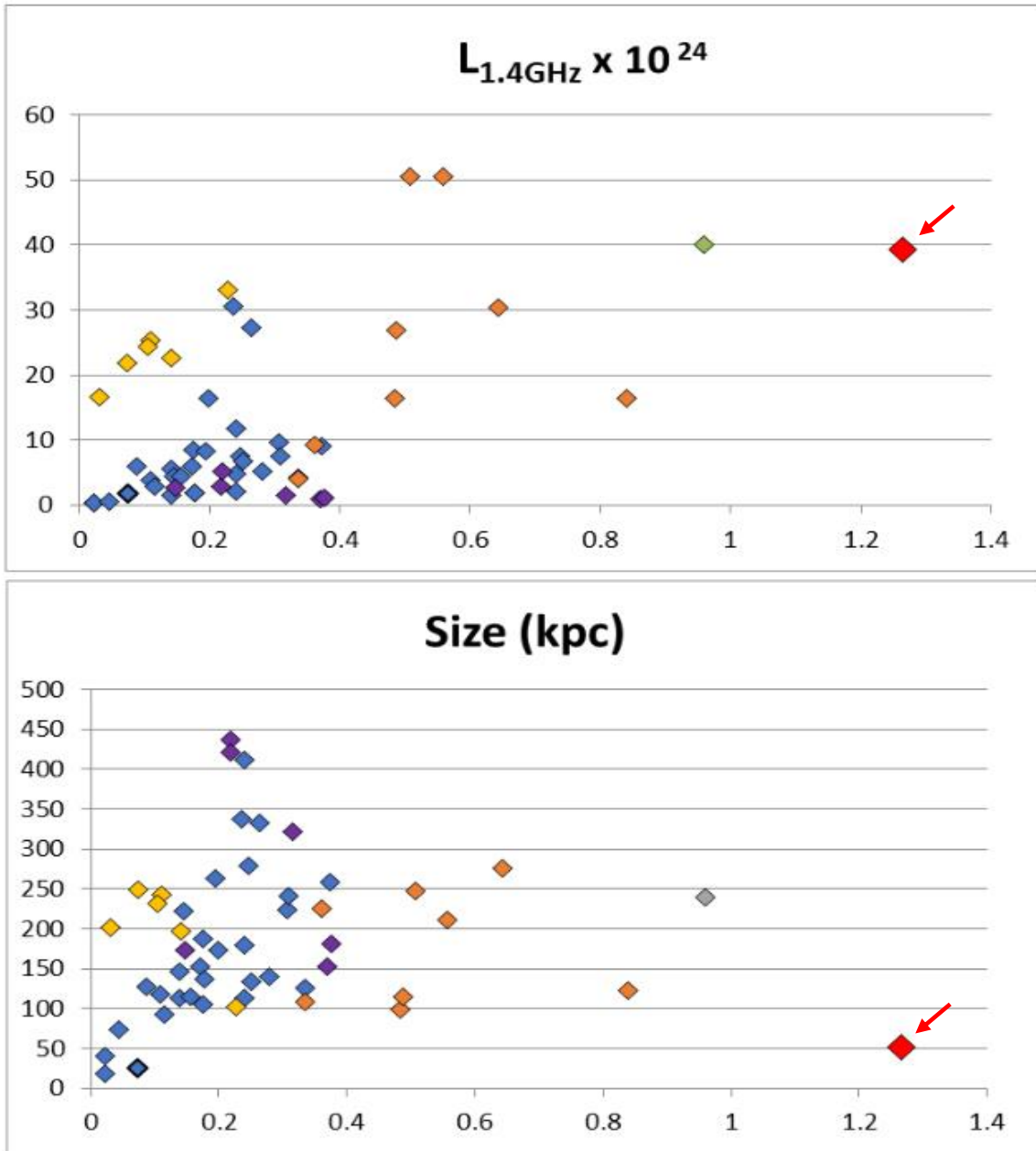
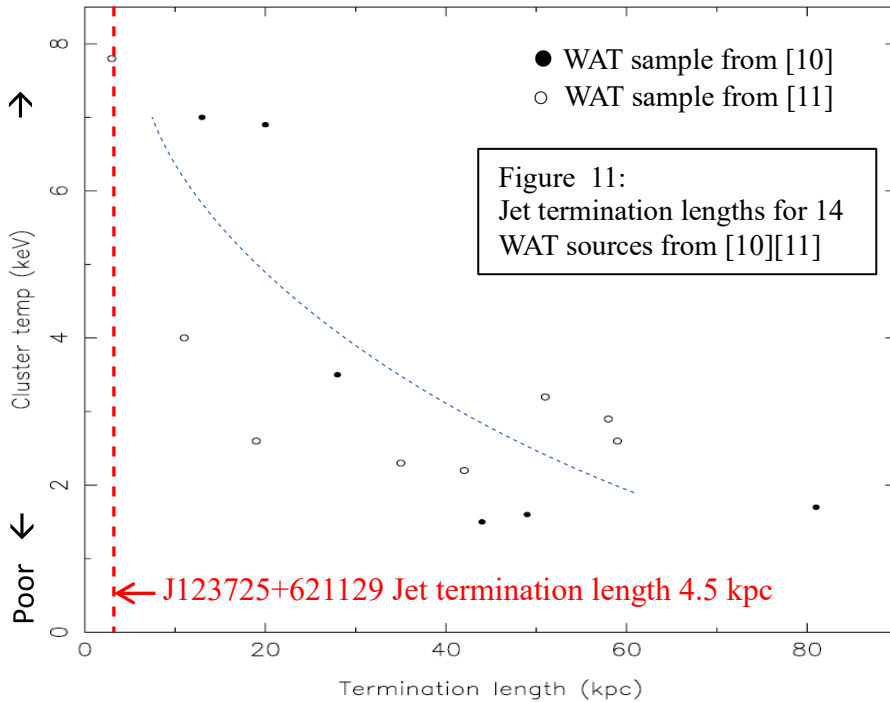


Figure 10: Properties of a representative sample of Wide-Angled-Tail radio source structures in the literature for comparison with J123725+621129 (arrowed). Sample drawn from [10][11][12][13][14]

As has already been noted, J123725+621129 is by comparison luminous but has a very small linear size. Figure 11 illustrates another WAT structural property – that of the jet termination length (the average core-inner hotspot linear separation). Hardcastle & Sakelliou (2004) [10] showed that for their sample the WAT jet termination length is related to the surrounding cluster

temperature - implying that hot cluster gas temperatures are associated with shorter jet termination lengths and disrupt outflowing WAT jets closer to the host galaxy.

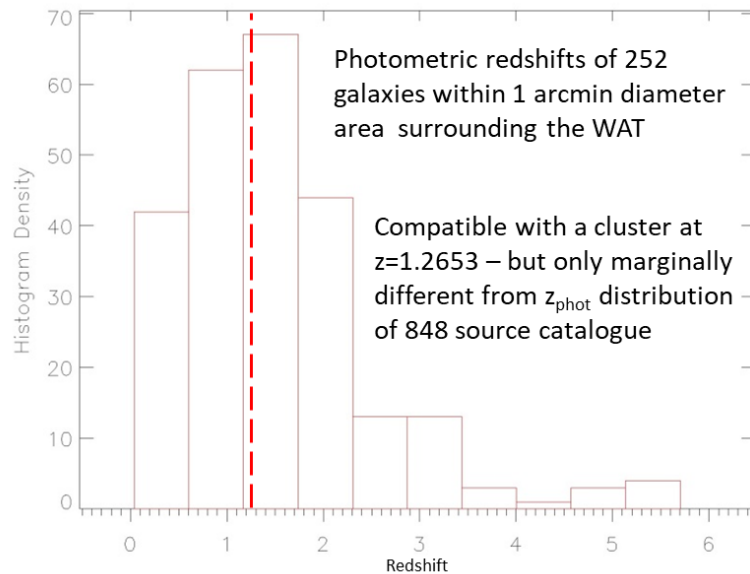
From Figure 8 it can be seen that J123725+621129 has a jet termination length of 4.5 kpc which



is very low in comparison with most WAT jet termination lengths and implies that cluster gas surrounding J12372+621129 is very hot with cluster gas temperatures ≤ 8 keV. WAT systems are usually associated with the dominant central elliptical galaxy in the centres of rich clusters. No X-ray emission is detected for this cluster, however the source probably lies at too high a redshift to get meaningful constraints on the X-ray intra-cluster gas from the Chandra non-detection (although though the host galaxy itself is detected).

Figure 12:
Photometric redshifts for the 252 galaxies within a 1 arcmin diameter area centred on J123725+621129

Figure 12 plots all the measured photometric redshifts for 252 galaxies within an area of 1 arcminute diameter centred on the Wide-Angled Tail radio source. The redshift distribution is statistically compatible with a large cluster at a redshift of 1.2653 but is statistically only marginally different from the photometric redshift distribution of the complete 848 e-MERGE source sample.



POS (EVN2022) 044

3. The e-MERGE Summary and Delivery Timescale

The e-MERGE radio survey is designed to image the μJy radio source population in great detail with nJy sensitivity and high angular resolution matching and exceeding that of the HST over arcsec to mas scales across the GOODS-N field. The full DR-2 release of the e-MERGE Survey will constrain models of star-formation and SMBH co-evolution, and study associated AGN feedback interactions within the host galaxies across cosmic time from over 4000 individual radio sources.

The high angular resolution the e-MERGE radio survey will be complementary to extremely wide field deep surveys of radio sources observed with other telescopes at lower angular resolution where the vast majority of the μJy radio source population remains essentially unresolved.

The e-MERGE science exploitation will utilise the extensive multi-band coverage across the GOODS-N field with the DR-2 release encompassing the HST multi-wavelength deep images (*HST CANDELS*).

The initial DR-1 images were released to the e-MERGE consortium membership in 2020 [1], and is in science exploitation for the brighter μJy radio sources within the central 15' of GOODS-N.

The DR-1.5 initial test combination imaging with VLBI (EVN) for AGN systems with the DR-1 release is under way and will be delivered on similar timescales to the DR2 full release.

The DR-2 full sensitivity image release to the consortium delivery expected in 2024 with science exploitation in 2024/25.

Acknowledgements

e-MERLIN is a National Facility operated by the University of Manchester at Jodrell Bank Observatory on behalf of STFC, part of UK Research and Innovation. The European VLBI Network is a joint facility of independent European, African, Asian, and North American radio astronomy institutes. Scientific results from data presented in this publication are derived from the following EVN project code: EG078.

4. References

- [1] T.W.B. Muxlow, et al., 2020, MNRAS 495, pp 1188-1208.
- [2] J.F. Radcliffe, et al., 2018, A&A 619, A48, pp. 1-14.
- [3] R.D. Baldi, A. Capetti, & F. Massaro, 2017, A&A 609 A1, pp. 1-10.
- [4] P. Padovani, et al., 2014, Multiwavelength AGN Surveys and Studies Proceedings IAU Symposium No. 304, A. Mickaelian, F. Aharonian & D. Sanders, eds..
- [5] A.P. Thomson, et al., *in prep*.
- [6] R.J. Ivison et al., 2010, MNRAS 402, pp. 245-258.
- [7] C.L. Carilli et al., 1991, ApJ 383, pp. 554-573.
- [8] V. Smolčić et al., 2007, ApJS, 172, pp. 295-313.
- [9] K.M. Blundell, & S. Rawlings, 2000, AJ, 119, pp. 1111-1122.
- [10] M.J. Hardcastle & I. Sakelliou, 2004, MNRAS, 349, pp. 560-575.
- [11] E.L. Blanton et al., 2000, ApJ, 531, pp. 118-136.
- [12] E.L. Blanton et al., 2001, AJ, 121, pp. 2915-2927.
- [13] E.L. Blanton et al., 2003, AJ, 125, pp. 1635-1641.
- [14] M.Y. Mao et al., 2010, MNRAS, 406, 2578-2590.
- [15] Blundell K. M., S. Rawlings S., C.J. & Willott, 1999, AJ, 117, 677-706.